Discover Applied Sciences

Research

Response surface optimization design of flexible positioning platform considering its fatigue life

Lufan Zhang[1] · Boshi Jiang[1] · Pengqi Zhang[1] · Heng Yan[1] · Hehe Sun[1]

Received: 23 July 2023 / Accepted: 11 March 2024
Published online: 15 March 2024

Abstract
The research of macro and micro motion platforms has always been committed to realizing the ultra-high acceleration operation of the platform and improving the positioning accuracy of the platform. With the goal of achieving ultra-high-speed, the impact of the increase in speed on key components has also attracted more and more attention. This paper takes a flexible positioning platform of an ultra-high acceleration macro–micro motion platform with adjustable voice coil motor (VCM) number and load as the research object. Perform static analysis, rigid-flexible coupled dynamic analysis, fatigue analysis, and multi-objective response surface optimization design (RSMD). The influence on the acceleration of the platform and the influence on the stress and fatigue life of the flexible positioning platform with the change of the number and load of the VCM were explored. The changes of the acceleration and speed curves of the platform during ultra-high-speed operation are obtained by dynamic analysis, and the position of the dangerous part of the flexible platform during operation is obtained. Finally, the RSMD is carried out to realize its performance optimization. The research conclusions of this paper have great reference value for the development of the macro–micro motion platform and the improvement of its structure.

Article Highlights

- The static analysis and dynamic analysis simulation of the flexible positioning platform are carried out.
- The fatigue life evaluation method is used to predict the fatigue life of the flexible positioning platform.
- The multi-objective response surface optimization method was used to optimize the flexible positioning platform.

Keywords Flexible positioning platform · Fatigue life · Dynamic analysis · RSMD

1 Introduction

The concept of the macro–micro composite drive is widely used in various motion platforms [1–5]. Many scholars have proposed research methods and theories on multi-drive and composite drives of macro–micro platforms, carried out in-depth research, and verified their performance. The two-dimensional macro–micro composite motion platform of Harbin Institute of Technology combines the cylindrical VCM and the piezoelectric ceramic structure. Through the analysis of static and dynamic characteristics, the acceleration can reach 5 g and the positioning accuracy is 21 nm [6]. Song Zekun [7] conducted

✉ Lufan Zhang, 89551677@qq.com | [1]School of Mechanical and Electrical Engineering, Henan University of Technology, Zhenzhou 450001, China.

control research on the macro–micro-structure workbench, studied the macro-movement structure and the micro-movement structure, achieved the predetermined accuracy, and reduced the influence of the interference force. Zhou [8] combined the VCM with the concept of macro–micro drive and studied the control of multi-axis motion controller for macro motion and the control analysis of VCM for micromotion. The positioning system developed by the Tokyo Institute of Technology is mainly composed of a ball screw and a brushed DC motor, and a gas static pressure table is used [9]. The maximum stroke of the platform can reach 400 mm, and the positioning accuracy can reach 4 nm under limited conditions. At present, many parts and equipment fail due to fatigue fracture, but few scholars have carried out fatigue analysis and research on key components of the macro–micro motion platform. In the aspect of fatigue research, there is a rich experience [10–13]. Fatigue analysis has been widely studied by scholars at home and abroad, and a large amount of experience and theoretical data have been accumulated. The understanding of fatigue problems has advanced very well in recent years, with numerous applications in roads, bridges, aerospace, and automotive. In foreign countries, Braithwaite [14] proposed the concept of metal fatigue in the nineteenth century. In 1920, Griffith [15] published a paper on the theory of brittle fracture, and fatigue fracture gradually began to develop. In 1945, Miner [16] proposed the linear fatigue cumulative damage theory, and the Miner criterion has been widely used. The research on fatigue analysis abroad has a long time and rich experience. In China, although the time is not too long, the development of fatigue has also been fruitful. In 1973, Gao [17] carried out the method of fatigue test. In 1977, Zhao [18] and others analyzed the fatigue damage of the top hammer of the six-sided top press and explained the stress state of the top hammer, fatigue fracture, and the causes and influencing factors of fatigue damage. In terms of application, domestic large-scale machinery such as cranes, excavators, and hydraulic presses have been widely used in fatigue analysis, and also in some small key components [19, 20]. To sum up, the research of domestic and foreign experts on the ultra-high-acceleration ultra-precision positioning motion platform mainly focuses on the structural design of the platform and the control of positioning accuracy. However, there are few studies on fatigue life prediction of the key devices of the platform under complex high-frequency start-stop, ultra-high acceleration actual conditions. Therefore, how to ensure the ultra-high life of the ultra-high-acceleration ultra-precision positioning motion platform is particularly important, and its fatigue life prediction is urgently needed. In the research of rigid-flexible coupling dynamics analysis of mechanical structures, predecessors have accumulated a lot of analysis experience, among which the key components of diesel engines have been analyzed by rigid-flexible coupling analysis by many scholars. Xu [21] calculated the stress distribution of the connecting rod in the operating cycle of the diesel engine by the method of rigid-flexible coupling analysis of the diesel engine connecting rod, compared it with the static analysis results and obtained the difference between the two calculations results. Fan [22] performed modal fatigue analysis on the ten sub-shafts in the transmission shaft, which was a related operation of fatigue analysis by obtaining modal stress files through rigid-flexible coupling analysis. In the optimization analysis of key components, the use of finite element software for size optimization has been used by many experts and scholars [23–25].

This paper mainly starts with the fatigue life prediction and optimization design of the key components of the macro and micro motion platform. Firstly, by changing the number of the VCM and the size of the load, the influence on the acceleration is explored. The static analysis of the flexible positioning platform is carried out to obtain the stress and deformation curve of the flexible positioning platform with the change of the number of the VCM. Then, according to the static analysis results and the S–N curve fatigue analysis, the influence of different VCM numbers on the macro–micro motion platform, then the dynamic analysis was carried out to obtain the dynamic characteristic cloud map and the stress cloud map of the flexible platform, and it was found that the stress value of the flexible hinge was larger. Finally, the flexible hinge is optimized by RSMD.

2 Flexible positioning platform

The macro–micro combined motion platform studied in this paper is an ultra-high-speed precision positioning platform. The positioning work is completed on a flexible platform. The flexible platform is divided into the macro-moving platform and the micro-moving platform. The main working process is that the VCM drives the connecting arm, the connecting arm drives the macro-movement platform to achieve macro-movement positioning, the piezoelectric driver drives the micro-movement platform to complete the micro-movement positioning, and the macro–micro combination completes ultra-high-speed and ultra-precision positioning work. This paper mainly explores the macro-motion positioning work of the macro–micro motion platform. The macro and micro motion platform model diagrams are shown in Fig. 1.

In Fig. 2, the number of the VCM is expanded to “n”, and platform the load is expanded to “m” kg. The acceleration of the motion platform is affected by the number of VCMs and the size of the load. The initial "n = 1, m = 6 kg (load)",

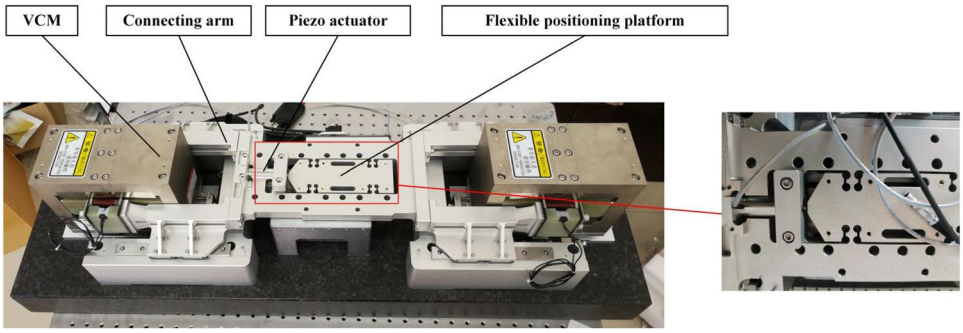

Fig. 1 Ultra-high acceleration macro–micro motion platform

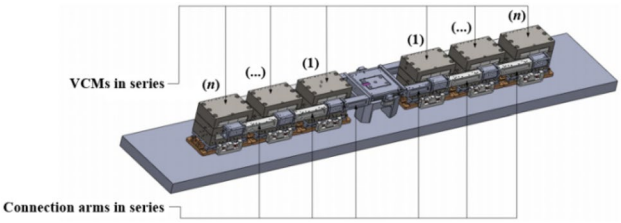

Fig. 2 Multi-level macro–micro motion platform [2]

the maximum acceleration is 300 m/s^2. From Newton's second law, we can know that under initial conditions, the thrust provided by VCM is 1800N, and the acceleration changes with the number and load of VCM pairs. It can be seen from Newton's second law that under initial conditions, VCM provides a thrust of 1800N, 900N on each side, and the acceleration varies with the number and load of VCM pairs. This is shown in Figs. 3 and 4, the acceleration curve of the flexible positioning platform as the VCM number and load change.

According to Newton's second law, under a certain load, the larger the number of VCMs, the greater the force provided by the motor and the greater the acceleration. In the case of a certain number of VCMs, the larger the load, the smaller the acceleration. As shown in Fig. 3, the red curve is the changing trend of acceleration when the load is 3 kg and remains unchanged, and the black curve is the changing trend of acceleration when the number of the VCM is "1" and remains unchanged.The left vertical axis is associated with the "platform quality" and the right vertical axis is associated with VCM. In Fig. 4, when the number of VCM pairs and the load both increase, the acceleration of the platform gradually increases, but as the VCM and the load increase to a certain extent, the change trend of the acceleration gradually decreases. It can be shown that when the number of VCM and the load is increased at the same time, the influence of the number of VCM on the acceleration of the platform is gradually weakened, and due to the limitation of the thrust provided by the VCM and the initial load, the final acceleration of the platform will not exceed 90 g (g = 9.8 m/s^2).

In this paper, static mechanical analysis, dynamic mechanical analysis, and fatigue analysis are carried out on the flexible positioning platform based on the change of the number of VCM and the load, so as to obtain the data of stress, deformation, fatigue life, acceleration and speed curve of the flexible positioning platform. The data cloud map is used to analyze and explore the influence of the VCM number and load on the flexible platform.

3 Mechanical analysis

In the calculation of engineering problems, people initially solve mathematical equations by calculating conditions and formulas, but in fact, many engineering problems have complex working conditions and boundary conditions, and in many cases can not find the final solution. With the development of science and technology, the finite element method is gradually applied to the solution of engineering problems. The analysis steps of finite element method include discretization of structure, determination of displacement function, analysis of element mechanical characteristics, establishment of node equilibrium equation, calculation of displacement analysis results and solution of element stress and strain.

The finite element model is built. The flexible positioning platform studied in this paper is established in SolidWorks, and the output is a file in "xt" format. It is imported into ANSYS Workbench for material assignment,

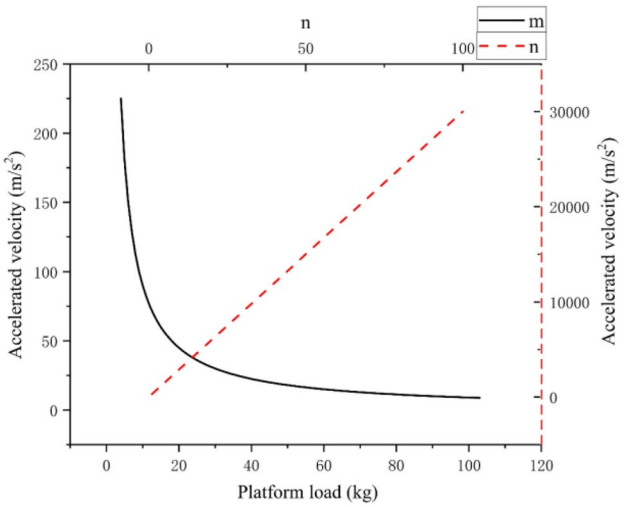

Fig. 3 2D relationship curve of platform mass and "n" to acceleration

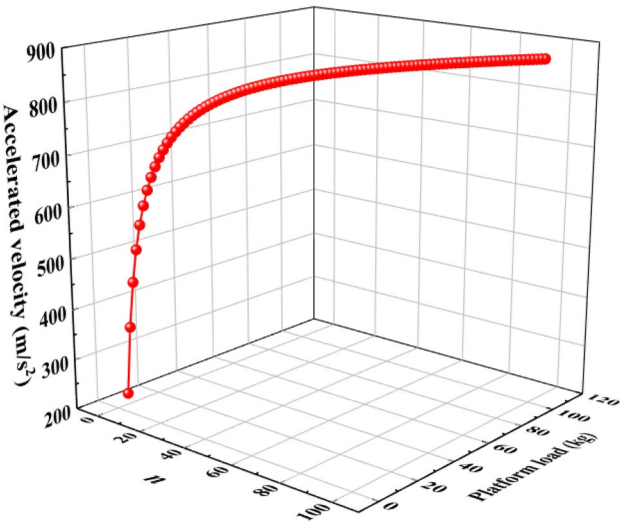

Fig. 4 3D relationship curve of platform mass and "n" to acceleration

boundary conditions, and load application. The constraints are fixed at the left end of the flexible platform, and the drive provided by the VCM is applied to the right segment to set the boundary conditions. The materials and boundary conditions used in the specific model are shown in Table 1 and Fig. 5.

Static analysis in Workbench is mainly divided into model import, material addition, mesh division and constraint addition, and output of stress and deformation results. Stress results can be used as preconditions for fatigue analysis. In this paper, when "n" is 1, the load provided by the voice coil motor is taken as the input condition. The obtained stress and deformation results are shown in Figs. 6 and 7.

It can be seen from the stress cloud diagram that the maximum stress is at the rounded corners between the two sides of the flexible positioning platform, and the maximum stress is 4.156×10^6 Pa. It can be seen that the location of the dangerous point is also here. When doing fatigue analysis, we should focus on the stress maximum area, which will be the lower life area. In the deformation cloud diagram, the closer to the force location, the greater the deformation, the constrained position has the lowest deformation, and the maximum deformation is 6.959×10^{-6} m on the right side of the flexible positioning platform, that is, at the force point.

As shown in Fig. 8, the deformation, stress, and force change curves of the flexible platform. It can be seen that both stress and deformation increase with increasing force. Among them, only when the number of the VCM changes, the thrust of the flexible platform will change, because the thrust of the flexible platform is provided by the VCM. When the number of VCM pairs is constant, the load increases while the thrust on the flexible platform remains constant. When both the load and the VCM number increase, the force change is also caused by the VCM number change.

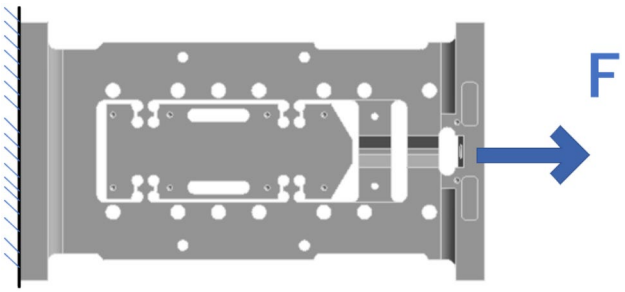

Fig. 5 Boundary conditions of the flexible positioning platform

Table 1 7075AL-T6 material list

Name	Numerical value	Unit
Young's modulus	7.1016×10^{10}	Pa
Poisson's ratio	0.33	–
Density	2793	Kg/m^3

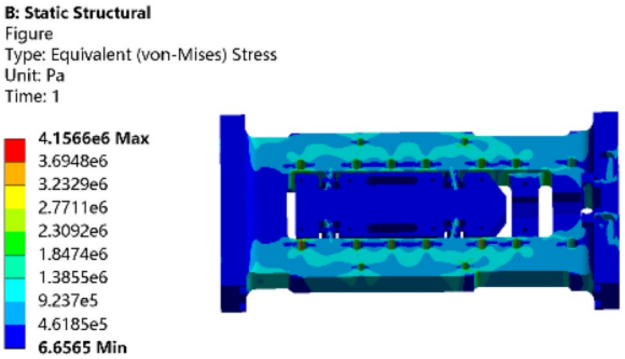

Fig. 6 Stress of the flexible positioning platform

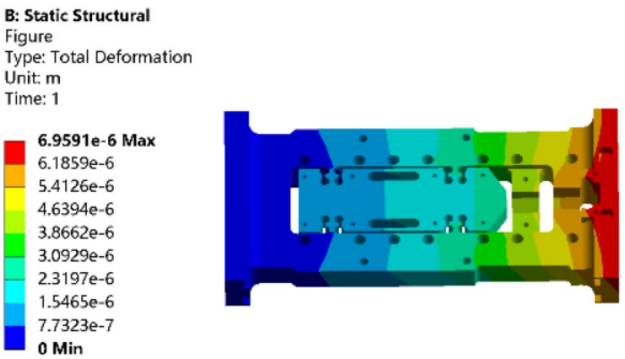

Fig. 7 Deformation of the flexible positioning platform

4 Fatigue analysis

The damage caused by the failure of mechanical parts every year is immeasurable, and fatigue fracture accounts for more than 50% of the failure [26]. Most of the main parts of construction machinery and railway bridges work under cyclically changing loads, and fatigue is the main failure form. In today's world, with the innovative development of the chip and semiconductor industries, the microelectronics manufacturing industry has led to a new wave of the industrial revolution. However, high-end manufacturing equipment and high-end chips in China's microelectronics industry still rely on imports. The macro–micro motion platform is the key equipment in the microelectronics manufacturing industry and is widely used in the field of ultra-precision positioning. The macro–micro motion platform is a complex reciprocating start-stop working

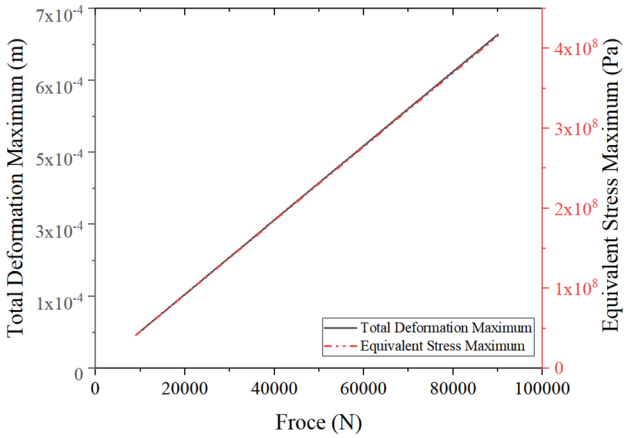

Fig. 8 Variation curve of stress and deformation with force

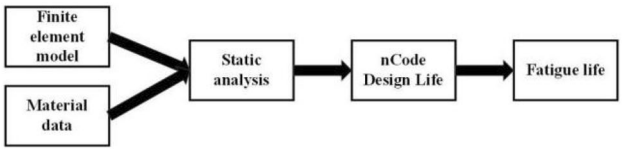

Fig. 9 Nominal stress method fatigue analysis process

device, working for a long time will inevitably cause fatigue. However, domestic and foreign researchers have little research on its fatigue life, mostly on the development of macro–micro motion platforms, the control of positioning accuracy, and the suppression of vibration. Therefore, it is urgent to predict the fatigue life of macro–micro motion platforms.

As shown in Fig. 9 is the analysis process of fatigue analysis in nCode. In this paper, the flexible platform is analyzed in nCode Design Life, and the fatigue life analysis is carried out by nCode Design Life based on the previous static analysis results. nCode Design Life is researched by nCode company and has been integrated into ANSYS Workbench. It is very easy to use the finite element analysis results in the workbench. nCode Design Life is very convenient to use and has powerful functions, including stress fatigue analysis, strain fatigue. Many modules such as analysis and random vibration fatigue analysis can also automatically generate load spectrum and S–N curve according to user needs, and can also use the optimization module of Workbench to optimize the life [27].

Fatigue analysis can be divided into a selection of fatigue analysis methods, solution of finite element analysis results, the input of S–N curve and load spectrum, and output of fatigue analysis results. There are many methods for fatigue analysis. Among them, the nominal stress method, the local strain method, and the stress field strength method are widely used. In this paper, the nominal stress method is used for fatigue analysis. The finite element analysis results are imported into nCode using the statics analysis results used previously. The load spectrum is the driving force provided by the VCM. Because the macro–micro motion platform is a reciprocating cycle, and the force on the flexible positioning platform is positive and negative, the calculation method of constant amplitude is selected in nCode. The S–N curve is extracted from the nCode material library.

As shown in Figs. 10 and 11, the fatigue damage and fatigue life cloud diagrams are obtained when "*n*" is 15. From the life and damage cloud diagrams, it can be seen that the position of the lowest point of life is the same as the position of the maximum stress in the static analysis.

As shown in Fig. 12, the relationship between the fatigue life of the flexible platform and the number of the VCM is listed. When "*n*" is less than 15, the fatigue life of the flexible platform is above 1×10^{15}, and when "*n*" is greater than 15, the fatigue life of the flexible platform is Below 1×10^{15}, with the increase of "*n*", the fatigue life gradually decreases. It can be considered that when "*n*" is large enough, the fatigue life of the flexible platform is very small, even zero. Therefore, when the number of the VCM increases, pay close attention to whether the fatigue life of the macro–micro motion platform meets the requirements. While increasing the acceleration of the platform, it is necessary to ensure that the macro and micro motion platform has an ultra-high service life and a long enough working time, so as to meet the original design intention of the macro and micro motion platform.

Fig. 10 Damage cloud map

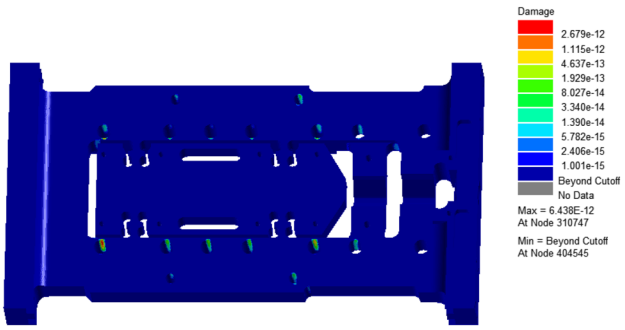

Fig. 11 Life cloud map

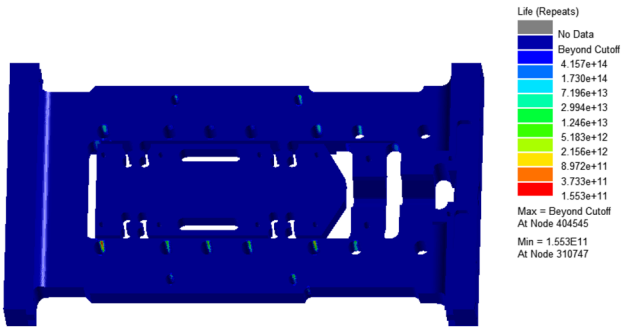

5 Rigid-flexible coupling dynamics analysis

When the flexible characteristics of the component change significantly under the precise deformation of the load, which affects the overall dynamic mechanical characteristics or action behavior of the model, the concept of a flexible body can be introduced [28].

The position of coordinates of each node of the flexible body is not fixed in the process of movement, and the flexible body is usually modeled by floating coordinate system. The floating coordinate system in the flexible multi-body system is shown in Fig. 13, including floating coordinate system (e^b) and inertial coordinate system (e^r). The floating coordinate system is built on the elastic body and moves with the deformation of the flexible body, which is used to represent the movement of the elastic body and changes with time. Inertial coordinate system refers to the global coordinate system, which does not change with time.

Because the ultra-high acceleration macro–micro motion platform operates at ultra-high speed, the flexible positioning platform will inevitably be hit by the connecting arm during the working process, and the impact will deform the flexible platform. working status. At present, there are many ways to convert parts into flexible bodies, which can be generated directly in Adams. First, the rigid body is constructed to be discretized, and then flexible beams are used to connect the various rigid body pieces to generate the required flexible bodies. This way Only for simple builds. The second is to generate a modal neutral file through the Adams/AutoFlex module of the flexible body module that comes with Adams. This method requires the establishment of a model in Adams. The third is to use finite element software to generate flexible bodies, such as ANSYS, Hypermesh, NASTRAN, etc., and then input them into Adams.

This paper uses the third method to generate a flexible body, which is to build a model in solid works, input it into HyperMesh, divide the mesh in HyperMesh, establish a rigid area, set material properties, and then perform modal settings and output MNF files used by Adams. The specific process is shown in Fig. 14.

In this multi-rigid body dynamics model, the connecting arm is connected to the flexible positioning platform, is located on the base, and is imported into Adams to add constraints and drives, this is shown in Fig. 15. The connecting arm moves linearly on the bottom plate driven by the VCM, the flexible platform is moved forward linearly by the thrust of the connecting arm, and the bottom plate remains fixed.

At the same time, add driving force to the voice coil motor, the acceleration to be achieved by the ultra-high acceleration macro micro motion platform is 300 m/s^2, the total mass of the flexible positioning platform, connecting arm and some accessories is about 6 kg, the driving force provided by Newton's second law can be obtained voice coil

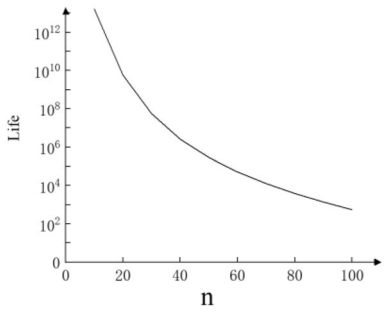

Fig. 12 Fatigue life with numberic deformation curve of VCM

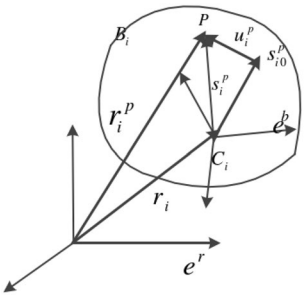

Fig. 13 Position of the "P" node of the flexible body

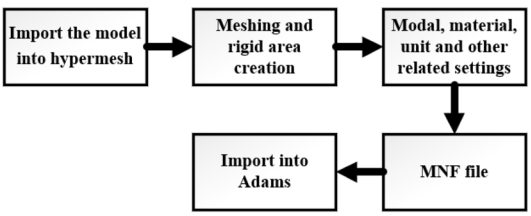

Fig. 14 "MNF" file generation process

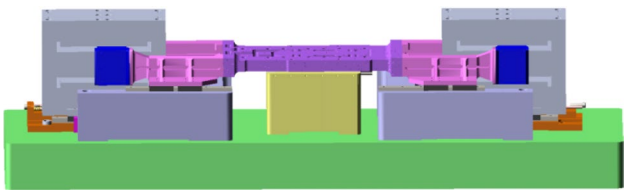

Fig. 15 Multi-rigid body model

motor is 1800N, and the driving force provided by the single-side voice coil motor is 900N, so the size of the forces on both sides in Adams is set to 900N (speed is equal to acceleration multiplied by time), and the running time is set to 0.01 s.

As shown in Fig. 16, the speed and acceleration of the flexible platform change with time, the speed increases with time, when the time is 0.01 s, the speed of the flexible platform is 3 m/s. In the acceleration curve, the acceleration size stabilization is about 300 m/s^2. This shows that the velocity and acceleration obtained in the rigid coupled kinetic model agree with the theoretical values, verifying the accuracy of the analysis.

As shown in Fig. 17, the flexible platform kinetic energy changes with time curve, known by the graph, the kinetic energy increases with time, from the kinetic energy and speed ($W = mv^2/2$), kinetic energy and speed is proportional, at 0.01, kinetic energy is 8.2 J, speed is 3 m/s^2, known flexible platform mass is about 1.8 kg, the theoretical value of 8.1 J, to the data and theoretical value.

It can be seen from Fig. 18 that the maximum stress is at the flexible hinge of the platform, and it can be known that when the flexible platform is hit instantaneously by the connecting arm, the impact on the flexible hinge is the largest.

During the micro-positioning of the macro–micro motion platform, the flexible hinge is driven by the piezoelectric actuator to complete the positioning work. During the micro-positioning work, the flexible hinge will be deformed, but this deformation will recover when no force is applied. The original position, so it can be seen that during the

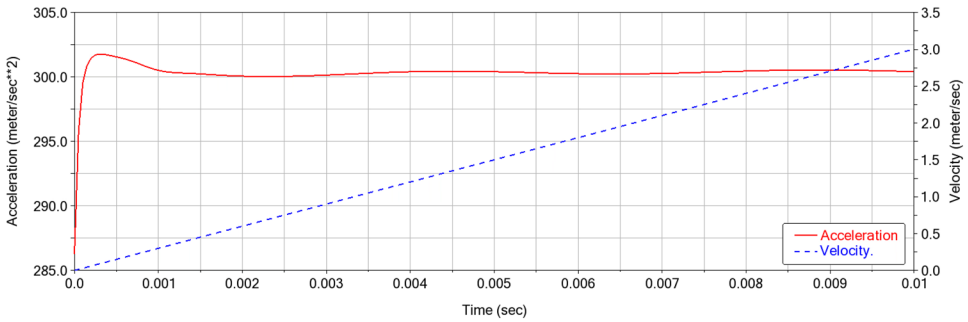

Fig. 16 Curves of acceleration and velocity versus time

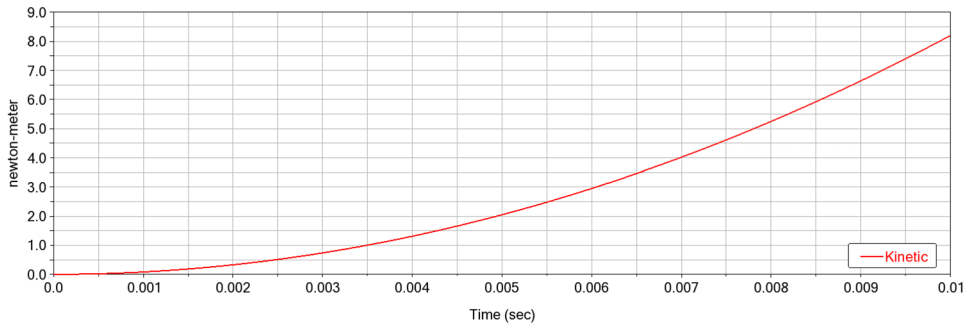

Fig. 17 Energy versus time curve

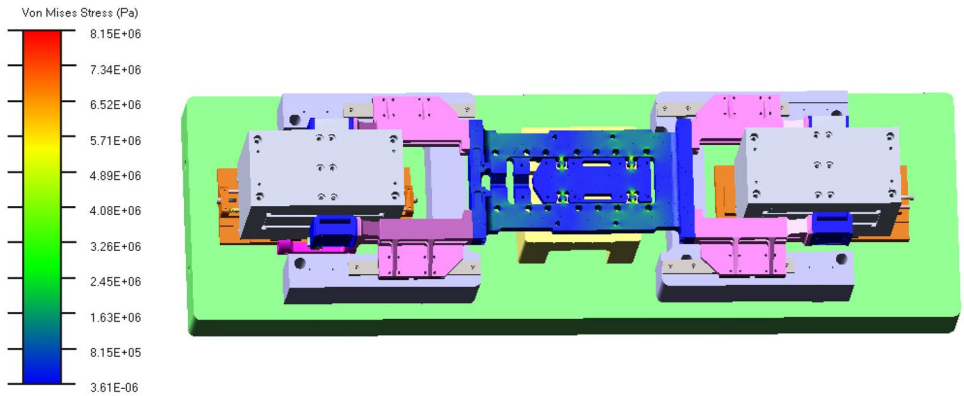

Fig. 18 Stress cloud diagram of the macro–micro motion platform

micro-positioning process, the dangerous part of the flexible positioning platform is at the flexible hinge, which can also be seen in the following analysis. The cloud diagram of the dynamic analysis results shows that the flexible hinge is also a dangerous part during the macro motion of the macro–micro motion platform, that is when the VCM drives the connecting arm to drive the flexible platform to complete the positioning work. Therefore, when optimizing, the flexible hinge can be one of the optimized positions.

6 Optimize the design

Optimal design is to obtain an optimal design scheme under the condition that the product meets the established requirements, which can not only cause no waste of materials but also maximize the function. In the previous dynamic analysis results, it can be obtained that when the flexible positioning platform is impacted by the connecting arm, the stress value of the flexible hinge part is the largest, and the phenomenon of stress concentration occurs. Therefore, the optimization model for this optimization is the flexible hinge part of the flexible positioning platform. The optimization goal is to achieve the minimum stress value without increasing its own weight or reducing its compliance. At the same time, in order to eliminate the influence of resonance phenomenon, the first order natural frequency of the flexible

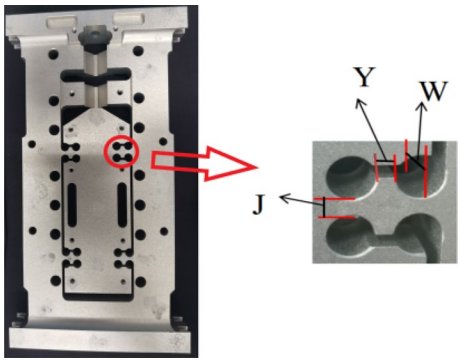

Fig. 19 Flexible positioning platform flexible hinge

positioning platform is minimized. The optimization method used is the response surface optimization in ANSYS Workbench.

Based on the above analysis, the response surface optimization mathematical model of the flexible hinge is as follows:

Find: $X_1;X_2;X_3;X_4;X_5\ldots\ldots X_n$.
Make: minδ(x), minσ(x), maxφ(x),max g(x); max h(x)。
δ(x): Maximum equivalent stress;
σ(x): Mass;
φ(x): Maximum deformation
g(x): Free mode first order natural frequency
h(x): Constrained mode first order natural frequency
Restraint: 10 mm ≤ X_1 = W ≤ 16 mm; 2 mm ≤ X_2 = J ≤ 6 mm; 2 mm ≤ X_3 = Y ≤ 6 mm.

In this paper, the distance and thickness between the two circles of the flexible hinge are used as optimization variables, and the optimization analysis is carried out in Workbench, this is shown in Fig. 19. First, the size of the flexible hinge optimization variable must be parameterized in SolidWorks. The specific method is to add "DS_" to the parameter prefix for Workbench identification, and then associate SolidWorks with ANSYS, transfer the data to Workbench through SolidWorks, mark the optimization variables in "DM" in Workbench, and perform finite element Analyze, mark the analysis results, and finally drag out the optimization module of Workbench for optimization analysis.

After completing the relevant operations in Solidworks, the finite element simulation of the model should be carried out in Workbench. This paper analyzes the statics of the flexible hinge and extracts the stress, deformation, and mass in the analysis results. The deformation and stress programs are shown in Figs. 20 and 21.

After the static analysis, the response surface optimization analysis is performed. The first step is to conduct the experimental design, which is used to collect data to calculate the response surface. There are many methods in experimental design, such as Central Composite Design, Optimal Space-Filling Design, Box-Behnken Design, Sparse Grid Initialization, and Latin Hypercube Sampling Design, etc. This paper chooses the default Central Composite Design, which is the most commonly used experimental design method, chooses Face-Centered in Samples Type, and chooses Enhanced in Template Type. The top 9 design points are shown in Table 2, and the variation curves of stress, deformation, and mass with sample points are shown in Figs. 22, 23, and 24.

After the experimental point calculation is completed, the construction of the response surface begins, and the selection of the appropriate response surface construction method can improve the accuracy of the response surface and reduce the error of the optimized design. For example, Genetic Aggregation, Standard Response Surface-Full 2nd Order Polynomials, Kriging, Non-Parametric Regression, Neural Network, and Sparse Grid, each with their own advantages and disadvantages, can be selected according to the needs of different methods. This paper chooses the Kriging method, which automatically adds design points to improve the accuracy of the response surface.

After the response surface is established, the fit degree chart and the fit degree curve can be generated, which can judge whether the established response surface model is accurate. As can be seen from Fig. 25 the design points on the fitting degree curve are also distributed on a line, indicating that the obtained response surface data is very accurate.

As shown in Figs. 26, 27, 28 and 29, 3D surface plot of optimization objectives and design variables. When J and Y are the horizontal and vertical coordinates of the surface graph, optimize the Z axis of the surface plot such as the effect force, the maximum deformation, and the mass of the surface plot, as shown in Fig. 26, the maximum equivalent force

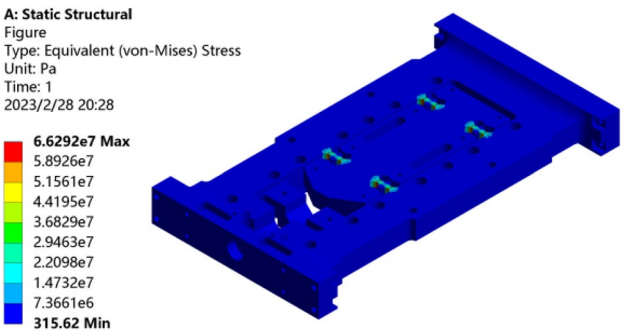

Fig. 20 Stress cloud diagram of the flexible platform

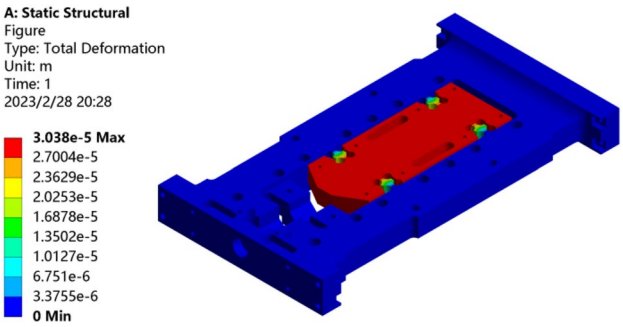

Fig. 21 Deformation cloud map of flexible hinge

Table 2 Optimal design of flexible positioning platform to generate sample point table

Name	J (mm)	Y (mm)	W (mm)	Maximum equivalent stress (Pa)	Maximum total deformation (m)	Geometry mass (kg)	Free mode first order natural frequency (Hz)	Constrained mode first order natural frequency (Hz)
1	4	4	13	4.85×10^{7}	2.24×10^{-5}	1.796	776.132	1158.50
2	2	4	13	4.25×10^{7}	1.73×10^{-5}	1.797	776.976	1164.69
3	3	4	13	4.54×10^{7}	1.97×10^{-5}	1.797	776.562	1161.67
4	6	4	13	5.54×10^{7}	2.85×10^{-5}	1.795	775.238	1151.60
5	5	4	13	5.2×10^{7}	2.53×10^{-5}	1.796	775.660	1155.12
6	4	2	13	1.57×10^{8}	8.65×10^{-5}	1.796	768.063	1076.95
7	4	3	13	7.73×10^{7}	3.78×10^{-5}	1.796	772.242	1147.95
8	4	6	13	3.44×10^{7}	1.20×10^{-5}	1.797	783.497	1174.28
9	4	5	13	3.97×10^{7}	1.56×10^{-5}	1.797	779.926	1167.10

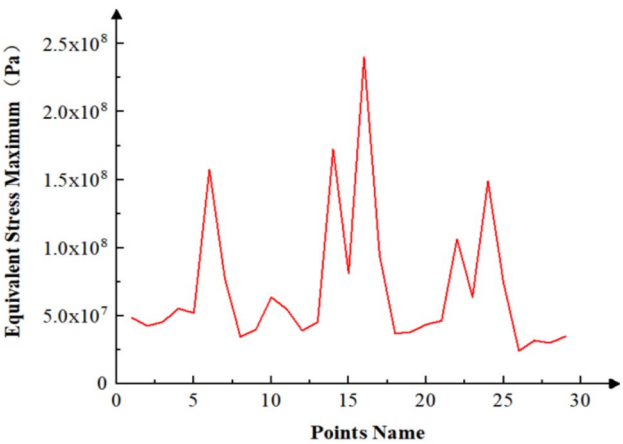

Fig. 22 Curve of stress versus sample point

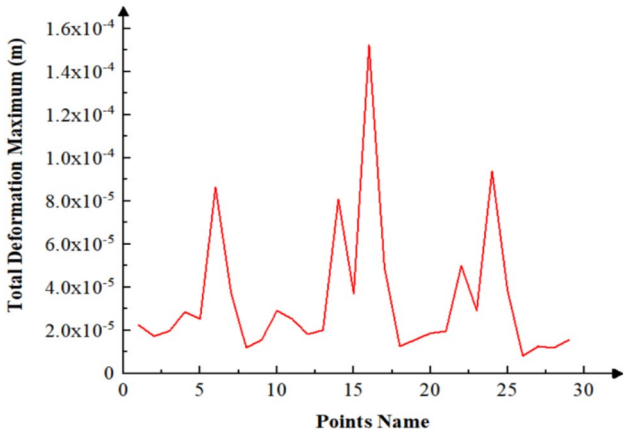

Fig. 23 Deformation curve with sample points

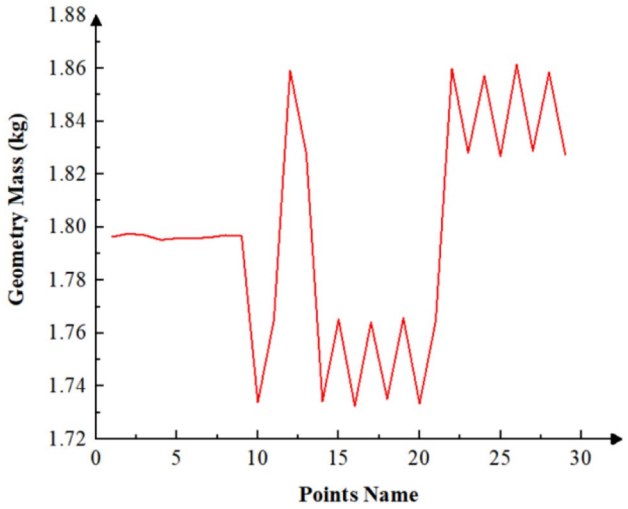

Fig. 24 Curve of mass change with sample point

changes from 3.0×10^{7} Pa to 1.9×10^{8} Pa, as shown in Fig. 27, the maximum deformation changes from 9.0×10^{-6} m to 1.2×10^{-4} m, As shown in Fig. 28, the mass varies from 1.795 to 1.798 kg. As shown in Fig. 29, the first-order natural frequency varies between 767 and 784 Hz.

As shown in Table 3, the three sets of optimal solutions generated by Workbench. After a comprehensive comparison and considering the actual situation, the size represented by the first group of design points is the final optimized size. Figures 30 and 31 are the maximum equivalent stress and maximum deformation cloud diagrams of the first scheme. The quality comparison results of stress and deformation before and after optimization are shown in Table 4.

The comparison data of stress, displacement and mass before and after optimization of the flexible positioning platform are shown in Table 4. After comparative analysis, the equivalent stress is reduced by 6.33% and the maximum displacement is increased by 0.33%, indicating that the optimization does not reduce the flexibility of the flexible positioning hinge, and the mass is reduced by 4.4%. Therefore, this optimization analysis has completed the optimization goal, that is, the equivalent stress and mass are reduced, and the compliance of the flexible hinge is not reduced. Compared with the original model, the utilization value of the flexible platform is greatly improved.

7 Conclusion

In this paper, the fatigue analysis and dynamic analysis of the macro motion condition of the flexible positioning platform are carried out, the dangerous parts under the micromotion condition are optimized and designed, and the following conclusions can be drawn.

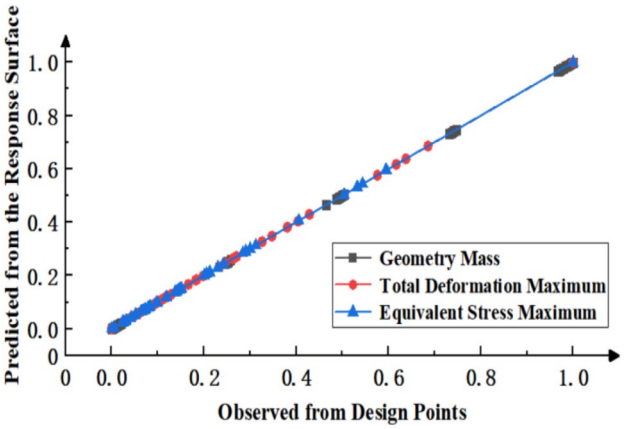

Fig. 25 The fit curve of response surface optimization

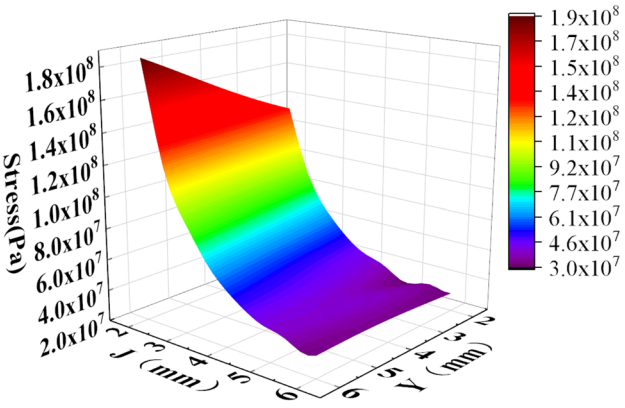

Fig. 26 Dimensions J and Y are plotted with equivalent stress surfaces

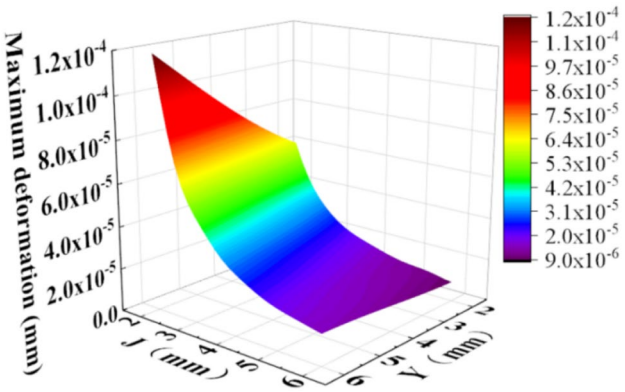

Fig. 27 Dimensions J and Y with maximum displacement surface plot

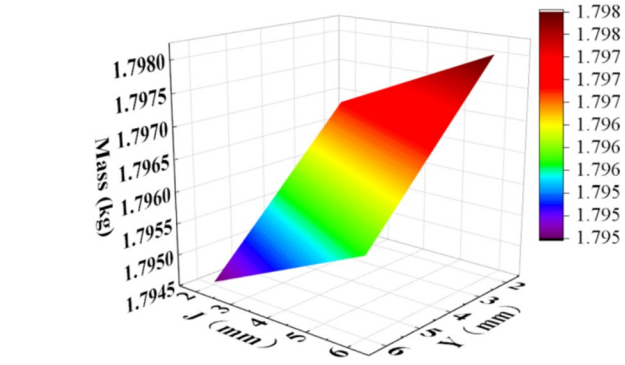

Fig. 28 Dimensions J and Y with quality surface diagram

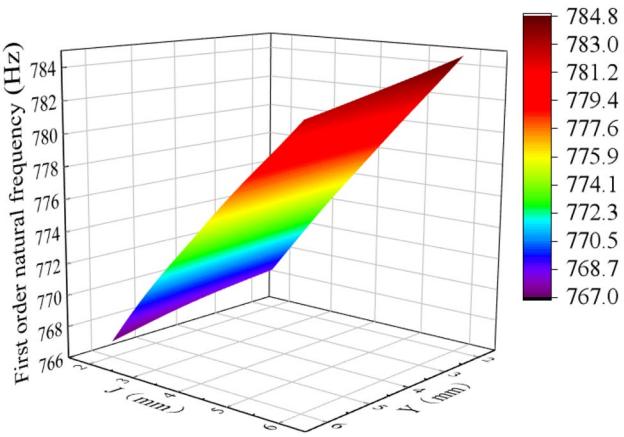

Fig. 29 Dimensions J and Y are analyzed with free-mode first-order natural frequency surface plots

Table 3 Optimize the program table

Name	J (mm)	Y (mm)	W (mm)	Equivalent stress maximum (Pa)	Total deformation maximum (m)	Geometry mass (kg)	Free mode first order natural Frequency (Hz)	Constrained mode first order natural frequency (Hz)
Candidate point 1	5.53	4.32	10.02	6.22×10^{7}	3.05×10^{-5}	1.73	786.68	1185.3
Candidate point 2	5.95	4.15	10.52	6.53×10^{7}	3.25×10^{-5}	1.74	784.12	1176.2
Candidate point 3	4.54	3.86	11.87	6.41×10^{7}	3.06×10^{-5}	1.75	782.75	1180.8

optimization are shown in Table 4.

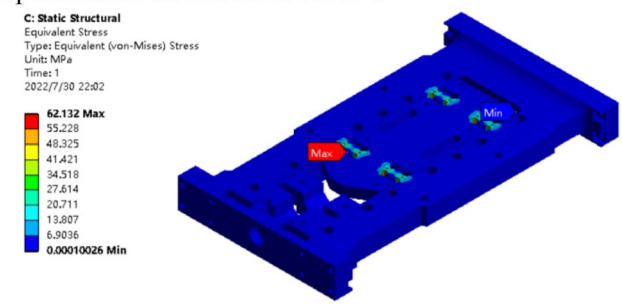

Fig. 30 The stress cloud diagram of the flexible platform after optimization

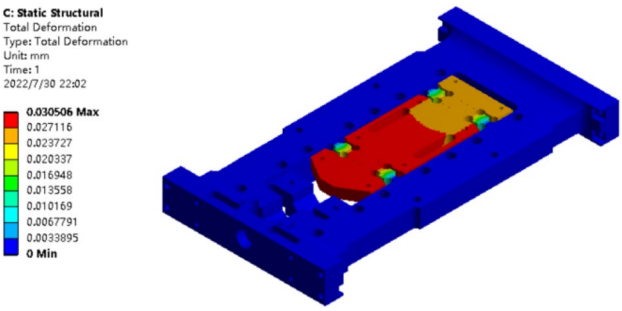

Fig. 31 The deformation cloud diagram of the flexible platform after optimization

1. Under the macro motion condition, increasing the number of VCM pairs is proportional to the acceleration of the macro and micro motion platform, and the load weight is inversely proportional to the acceleration. The fatigue life of the flexible positioning platform will decrease with the increase of the number of the VCM. When the number of the VCM increases to a certain extent, the fatigue life of the flexible platform will be reduced to zero.

Table 4 Comparison of results before and after optimization of flexible positioning platform

Optimization objective	Before optimization	Optimized	Elevate (%)
Equivalent stress maximum (Pa)	6.63×10^{7}	6.21×10^{7}	−6.33
Total deformation maximum (m)	3.04×10^{-5}	3.05×10^{-5}	+0.33
Geometry mass (kg)	1.82	1.74	−4.4
Free mode first order natural Frequency (Hz)	769.10	786.64	+2.3
Constrained mode first order natural frequency (Hz)	1140.20	1187.20	+4.1

2. In the dynamic analysis of rigid-flex coupling of macro-micromotion platform, the acceleration curve and velocity and kinetic energy of the flexible positioning platform with time are obtained. It is concluded that when the connecting arm drives the flexible platform, the flexible hinge is stressed the most and is the dangerous part.
3. In the RSMD of the flexible hinge, its equivalent stress and mass are reduced, and the flexibility of the flexible hinge is increased, thereby increasing the utilization value of the flexible positioning platform and reducing the cost.

Acknowledgements This research was financially supported by China Postdoctoral Science Foundation, the National Natural Science Foundation of China (Grant No. 51705132), the Natural Science Project of Henan Provincial Department of Science and Technology (Grant No. 222102220088) and the Natural Science Project of Henan Provincial Department of Education (Grant No. 21A460006).

Author contributions A and B wrote the main manuscript text, and C, D and E prepared the literature review part of the paper. All the authors reviewed the manuscript. (A:lufan zhang; B:boshi jiang; C:pengqi zhang; D:heng yan;E: hehe zhang)

Funding This research was financially supported by China Postdoctoral Science Foundation, the National Natural Science Foundation ofChina (Grant No. 51705132), the Natural Science Project of Henan Provincial Department of Science and Technology (Grant No.222102220088) and the Natural Science Project of Henan Provincial Department of Education (Grant No. 21A460006).

Data availability Data sharing not applicable to this article as no datasets were generated or analysed during the current study.

Declarations

Competing interests The authors declare no competing interests.

References

1. Chen JS, Dwang IC. A ballscrew drive mechanism with Piezo-electric nut for Preload and motion control. Mach Tool Manuf. 2000;40(4):513–26. https://doi.org/10.1016/S0890-6955(99)00078-4.
2. Zhang LF, Li XL, Fang JW, Lv YH, Ma B, Wu J, Li H. Vibration isolation of extended ultra-high acceleration macro-micro motion platform considering floating stator stage. Int J Precision Eng Manuf. 2019;20:1265–87. https://doi.org/10.1007/s12541-019-00152-7.
3. Zeng DP, Huang RR, Yang ZJ, Xue WC. Frequency response analysis of macro-micro stages with active disturbance reject controller. In: Proceedings of the ASME design engineering technicalconference, vol. 9 (2019). https://doi.org/10.1115/DETC2019-98352
4. Shi X, Wei YG. Research on bidirectional macro-micro assembly technology accuracy based on 3-UPU parallel mechanism. In Proceedings of 2018 IEEE international conference on mechatronics and automation, ICMA, pp. 1411–1416 (2018). https://doi.org/10.1109/ICMA.2018.8484641
5. Li XL, Zhang LF, Jiang BS, Fang JW, Zheng YX. Research trends in China for macro-micro motion platform for microelectronics manufacturing industry. J Adv Mech Des Syst Manuf. 2021. https://doi.org/10.1299/jamdsm.2021jamdsm0032.
6. Jie DG. Research on macro/micro-driven high-speed and high-precision positioning system, Ph.D. thesis, Harbin Institute of Technology (2006) (**in Chinese**).
7. Song ZK. Research on modeling and control methods of macro and micro composite precision motion platform. M.S. thesis, Harbin Institute of Technology (2020) (**in Chinese**).
8. Zhou WB. Development of macro/micro platform control system based on VCM, MS.thesis, Guangdong University of Technology (2014) (**in Chinese**).

9. Zhang LY. Research on vibration suppression and precise positioning method of high-speed and large-stroke macro-micro composite motion platform. Ph.D. thesis, Guangdong University of Technology (2018) (**in Chinese**).
10. Raftar HR, Dabiri E, Ahola A, Björk T. Weld root fatigue assessment of load-carrying fillet welded joints: 4R method compared to other methods. Int J Fatigue. 2022. https://doi.org/10.1016/j.ijfatigue.2021.106623.
11. Xiao GJ, Sha ZJ, Sha PB, Chen BQ, Li SC, Zhuo XQ. Fatigue life analysis of aero-engine blades for abrasive belt grinding considering residual stress. Eng Fail Anal. 2022;131:105846. https://doi.org/10.1016/j.engfailanal.2021.105846.
12. Zhao XY, Xie SQ, Zhang YL, Li Q, Wang WJ, Wang BJ. Fatigue reliability analysis of metro bogie frame based on effective notch stress method. Eng Fail Anal. 2022;131:105811. https://doi.org/10.1016/j.engfailanal.2021.105811.
13. Wu SF, Kang M, Cai ZW, Wang WZ. Multi-axial creep-fatigue analysis of a cracked groove structure subjected to cyclic thermal loading. Eng Fail Anal. 2022;131:105826. https://doi.org/10.1016/j.engfailanal.2021.105826.
14. Braithwaite F. On the fatigue and consequent fracture of metals. Min Proc Inst Civil Eng. 1854;13:1854. https://doi.org/10.1680/imotp.1854.23960.
15. Lu LT, Zhang WH. Review of research on very high cycle fatigue of metal materials. J Mech Strength 388–394; 2005 (**in Chinese**).
16. Miner MA. Cumulative damage in fatigue. Appl Mech. 1945. https://doi.org/10.1115/1.4009458.
17. Gao ZT. An overview of "fatigue test methods and analysis of test results". In: Presented at 708 fatigue conference. Physical and chemical testing, Physical Testing and Chemical Analysis(Part A:Physical Testing), pp. 22–27 (1974) (**in Chinese**)
18. Zhao YL. Preliminary analysis of fatigue failure of hex top hammer. Artif Diamond 1976;1–15+38–39 (**in Chinese**)
19. Chen YL, Long YP, Sheng TY, Li WQ. Fatigue analysis and optimization design of cutter disk shaft ofsugarcane harvester. J Agric Mech Res 2021;43(1):8–13+18 (**in Chinese**)
20. Wang Z, Wang L, Nie CH, Ma ZM, Wang Z, Xiao JP. Vibration fatigue analysis and test verification of theexternal spare wheel bracket. Veh Power Technol 2020;25–29 (**in Chinese**)
21. Xu ZJ. Finite element analysis of connecting rod of diesel engine, MS.thesis, Dalian Jiaotong University (2020) (**in Chinese**).
22. Liu ZG. Lightweight design of the open pre-bending machine based on FEA, MS.thesis, Qingdao University (2019) (**in Chinese**).
23. Wang HM. Finite element analysis and structural optimization design of key components of winding machine. MS.thesis, Shandong Architecture University (**in Chinese**) (2019).
24. Zhang KT. Finite Element Analysis and Lightweight Design of Gantry 8000 Bender. MS.thesis, Qingdao University (2019) (**in Chinese**).
25. Wang JW. Research on conventional fatigue strength design method of mechanical parts. Modern manufacturing technology and equipment, pp. 77–78 (2016) (**in Chinese**)
26. Fu SS. ANSYS nCode DesignLife fatigue analysis fundamentals and example tutorials. People Post Press (2020) (**in Chinese**).
27. Ma J, Wang ZT, Zhou D, Liao LH, Huang Z. Analysis of wind-induced vibration and fatigue effects of a typical tower crane. J Shanghai Jiaotong Univ (Chin Ed). 2014;68:804–8.
28. Han CR. Fatigue life analysis of tower cranes based on rigid-flexible coupled dynamics simulation. MS.thesis, Beijing University of Civil Engineering and Architecture (2021) (**in Chinese**).